Contribution from the Departments of Chemistry, West Virginia University, Morgantown, West Virginia 26506, and Brandeis University, Waltham, Massachusetts 02254

Structures of the Homologous Series of Square-Planar Metallotetrapyrroles Palladium(II) Octaethylporphyrin, Palladium(II) *trans*-Octaethylchlorin, and Palladium(II) *tct*-Octaethylisobacteriochlorin

Alan M. Stolzenberg,*,† Leonard J. Schussel,† Jack S. Summers,† Bruce M. Foxman,‡ and Jeffrey L. Petersen†

Received September 9, 1991

The molecular structures of a homologous series of palladium(II) porphyrin, chlorin, and isobacteriochlorin complexes were determined by X-ray diffraction. The porphyrin compound (2,3,7,8,12,13,17,18-octaethylporphyrinato)palladium(II), Pd(OEP), crystallizes in the triclinic space group $P\bar{1}$ ($Z = 1$) with unit cell dimensions $a = 7.809$ (5) Å, $b = 9.934$ (4) Å, $c = 10.429$ (3) Å, $\alpha = 91.05$ (2)°, $\beta = 98.07$ (4)°, $\gamma = 111.05$ (4)°, and $V = 745.4$ (5) Å^3. The structure has been refined to $R = 0.057$ on F_o on the basis of 3437 reflections with $F_o^2 > 0$. Pd(OEP) has a crystallographically imposed inversion center. The chlorin compound (*trans*-2,3-dihydro-2,3,7,8,12,13,17,18-octaethylporphyrinato)palladium(II), *t*-Pd(OEC), crystallizes in the orthorhombic space group *Pnab* ($Z = 4$) with unit cell dimensions $a = 8.969$ (3) Å, $b = 15.867$ (5) Å, $c = 22.117$ (7) Å, and $V = 3147.5$ (3.0) Å^3. The structure has been refined to $R = 0.0358$ on F_o on the basis of 1671 reflections with $I > 1.96\sigma(I)$. Pd(OEC) has a crystallographically imposed 2-fold axis passing through the unique pyrroline nitrogen atom, the palladium atom, and the pyrrole nitrogen which is across the macrocycle from the pyrroline ring. The isobacteriochlorin compound (*tct*-2,3,7,8-tetrahydro-2,3,7,8,12,13,17,18-octaethylporphyrinato)palladium(II), *tct*-Pd(OEiBC), crystallizes in the monoclinic space group $P2_1/n$ ($Z = 4$) with unit cell dimensions $a = 12.540$ (4) Å, $b = 12.745$ (3) Å, $c = 20.557$ (6) Å, $\beta = 92.24$ (2)°, and $V = 3283$ (1.5) Å^3. The structure has been refined to $R = 0.056$ on F_o on the basis of 4005 reflections with $F_o^2 > 3\sigma(F_o^2)$. Bond distances and angles in Pd(OEiBC) nearly exhibit mirror symmetry, even though no symmetry is imposed by the lattice. The conformation of the macrocycles in the three structures is either planar (OEP) or slightly ruffled. The ruffling appears to result primarily from packing interactions (OEC) or from the intrinsic ligand conformation that is a consequence of steric interactions between peripheral substituents (OEiBC) rather than from a drive to reduce M-N distances as in the case of nickel. Pd-N distances in this series are close to or slightly longer than the M-N distance for Hoard's reference porphyrin of least strain. Average Pd-N distances are 2.014 (4) Å for Pd(OEP), 2.016 (4) Å (pyrrole) and 2.039 (4) Å (pyrroline) for Pd(OEC), and 2.020 (6) Å (pyrrole) and 2.030 (5) Å (pyrroline) for Pd(OEiBC). The densities of these solids decrease or equivalently the volume per molecule increases with increasing saturation of the macrocycles. This trend appears to be general for β-substituted and ruffled hydroporphyrins.

Interest in the structural features of hydroporphyrins has been heightened by the recognition that the physical properties and reactivity of these compounds are affected by their conformation. Functional significance is attributed to the nonplanar conformations of the tetrapyrrole prosthetic groups in B_{12}-dependent enzymes,[1] the F_{430}-containing enzyme methylcoenzyme-M reductase,[2] and photosynthetic reaction centers.[3] Theoretical calculations suggest that changes in the conformation of tetrapyrroles alter the energies of the highest occupied and lowest unoccupied molecular orbitals and consequently affect spectroscopic and redox properties.[3,4] Porphyrins distorted by severe peripheral crowding have properties that are consistent with these calculations.[5] The influence of tetrapyrrole conformation on reactivity is demonstrated by the enhanced stability that the ruffled conformation of *cis*-Ni(OEC) affords its cation radical.[6] We proposed that the hole size of a tetrapyrrole and the ease with which its conformation can be varied can control the accessibility of oxidation states and/or spin states of a coordinated metal ion and can influence ligand-binding equilibria.[7] Interestingly, nickel hexahydro- and octahydroporphyrins, although reduced at more negative potentials than nickel isobacteriochlorins, do not yield Ni(I) species like the isobacteriochlorin.[8] It is thought that these more saturated tetrapyrroles are not sufficiently flexible to accommodate the structural distortions that occur upon formation of Ni(I).

The number of structures of free-base hydroporphyrin and metallohydroporphyrin compounds that have been reported[9-13] is sufficient for several trends to be apparent.[14] Hydroporphyrins have substantially greater conformation flexibility than porphyrins. Deviations from the mean plane of a hydroporphyrin can be quite large. This is a statement of possibility rather than of necessity, though. Free-base isobacteriochlorins with both planar[12] and nonplanar[13a] cores have been observed. In contrast, nickel hydroporphyrin complexes invariably exhibit a marked S_4 ruffle and are saddle-shaped.[10,13] The steepness of the saddle increases with the degree of saturation of the macrocycle π-system, and the Ni-N(pyrrole) and Ni-N(pyrroline) bond lengths both decrease.

† West Virginia University.
‡ Brandeis University.

(1) Geno, M. K.; Halpern, J. *J. Am. Chem. Soc.* **1987**, *109*, 1238.
(2) (a) Eschenmoser, A. *Ann. N.Y. Acad. Sci.* **1986**, *471*, 108. (b) Furenlid, L. R.; Renner, M. W.; Smith, K. M.; Fajer, J. *J. Am. Chem. Soc.* **1990**, *112*, 1634. (c) Furenlid, L. R.; Renner, M. W.; Fajer, J. *J. Am. Chem. Soc.* **1990**, *112*, 8987.
(3) Barkigia, K. M.; Chantranupong, L.; Smith, K. M.; Fajer, J. *J. Am. Chem. Soc.* **1988**, *110*, 7566.
(4) Gudowska-Nowak, E.; Newton, M. D.; Fajer, J. *J. Phys. Chem.* **1990**, *94*, 5795.
(5) (a) Medforth, C. J.; Berber, M. D.; Smith, K. M.; Shelnutt, J. A. *Tetrahedron Lett.* **1990**, *31*, 3719. (b) Barkigia, K. M.; Berber, M. D.; Fajer, J.; Medforth, C. J.; Renner, M. W.; Smith, K. M. *J. Am. Chem. Soc.* **1990**, *112*, 8851.
(6) Stolzenberg, A. M.; Stershic, M. T. *Inorg. Chem.* **1988**, *27*, 1614.
(7) Stolzenberg, A. M.; Stershic, M. T. *J. Am. Chem. Soc.* **1988**, *110*, 6391.
(8) Renner, M. W.; Furenlid, L. R.; Barkigia, K. M.; Forman, A.; Shim, H.-K.; Simpson, D. J.; Smith, K. M.; Fajer, J. *J. Am. Chem. Soc.* **1991**, *113*, 6891.
(9) (a) Spaulding, L. D.; Andrews, L. C.; Williams, G. J. B. *J. Am. Chem. Soc.* **1977**, *99*, 6918. (b) Barkigia, K. M.; Fajer, J.; Spaulding, L. D.; Williams, G. J. B. *J. Am. Chem. Soc.* **1981**, *103*, 176. (c) Barkigia, K. M.; Miura, M.; Thompson, M. A.; Fajer, J. *Inorg. Chem.* **1991**, *30*, 2233.
(10) (a) Ulman, A.; Galluci, J.; Fisher, D.; Ibers, J. A. *J. Am. Chem. Soc.* **1980**, *102*, 6852. (b) Galluci, J. C.; Swepston, P. N.; Ibers, J. A. *Acta Crystallogr., Sect. B* **1982**, *B38*, 2134. (c) Suh, M. P.; Swepston, P. N.; Ibers, J. A. *J. Am. Chem. Soc.* **1984**, *106*, 5164.
(11) (a) Strauss, S. H.; Silver, M. E.; Ibers, J. A. *J. Am. Chem. Soc.* **1983**, *105*, 4108. (b) Strauss, S. H.; Silver, M. E.; Long, K. M.; Thompson, R. G.; Hudgens, R. A.; Spartalian, K.; Ibers, J. A. *J. Am. Chem. Soc.* **1985**, *107*, 4207. (c) Strauss, S. H.; Pawlik, M. J.; Skowyra, J.; Kennedy, J. R.; Anderson, O. P.; Spartalian, K.; Dye, J. L. *Inorg. Chem.* **1987**, *26*, 724.
(12) Cruse, W. B. T.; Harrison, P. J.; Kennard, O. *J. Am. Chem. Soc.* **1982**, *104*, 2376.
(13) (a) Kratky, C.; Angst, C.; Johansen, J. E. *Angew. Chem., Int. Ed. Engl.* **1981**, *20*, 211. (b) Johansen, J. E.; Piermattie, V.; Angst, C.; Diener, E.; Kratky, C.; Eschenmoser, A. *Angew. Chem., Int. Ed. Engl.* **1981**, *20*, 261. (c) Kratky, C.; Waditschatka, R.; Angst, C.; Johansen, J. E.; Plaquevent, J. C.; Schreiber, J.; Eschenmoser, A. *Helv. Chim. Acta* **1985**, *68*, 1312. (d) Waditschatka, R.; Kratky, C.; Jaun, B.; Heinzer, J.; Eschenmoser, A. *J. Chem. Soc., Chem. Commun.* **1985**, 1604.
(14) Scheidt, W. R.; Lee, Y. J. *Struct. Bonding (Berlin)* **1987**, *64*, 1.

0020-1669/92/1331-1678$03.00/0

Ruffling results from the mismatch of the M–N bond lengths that are optimal for square-planar, low-spin Ni(II) and for planar porphyrin and hydroporphyrin macrocycles. An S_4 ruffle can decrease the M–N bond distances.[15] Hydroporphyrins are believed to have intrinsically larger core sizes.[10c,11,15] Apparently, the more saturated hydroporphyrins must ruffle more steeply to compensate for their larger cores. Ruffling is not expected to be as prevalent for complexes of metals with larger ionic radii. Other trends observed relate to bond lengths. The C_b–C_b and C_a–C_b bond lengths increase on saturation of the pyrrole ring. Saturation of one or more pyrrole rings results in an increased M–N bond distance to the pyrroline ring(s). However, as the number of reduced rings increases, the differences in the M–N(pyrrole) and M–N(pyrroline) distances appear to decrease. Unfortunately, the available data are from structures in the Zn(TPP),[9] Ni(TMP),[10] and Ni(OEP)[13] series. The zinc complexes are five-coordinate with slightly saddle-shaped macrocycles. The nickel complexes are ruffled and have short M–N bond distances. Both structure types permit adjustments that allow for closer equivalence of the M–N bond distances. A proper test of the number of reduced rings on M–N bond distances requires additional structural data for square-planar complexes of metals with larger ionic radii.

We report here the structures of the homologous series of square-planar Pd(II) complexes Pd(OEP), Pd(OEC), and *tct*-Pd(OEiBC). The difference between Pd–N(pyrrole) and Pd–N(pyrroline) bond lengths becomes less pronounced as the number of reduced rings increases in this series. However, this trend may not be a simple correlation with the number of saturated rings. We also note a previously unrecognized trend. The density of crystalline hydroporphyrins decreases or equivalently the volume per molecule increases with the degree of saturation of the π-system. This phenomenon may potentially result in significant differences in the chemistries of porphyrin and of hydroporphyrin compounds.

Experimental Section

Pd(OEP), Pd(OEC), and Pd(OEiBC) were prepared as previously reported.[16] Crystals of Pd(OEP) were grown by slow cooling of a hot xylene solution. Pd(OEC) was recrystallized by layering methanol over a chloroform solution of the complex. Crystals of Pd(OEiBC) were obtained from benzene/ethanol. Several repetitions of the recrystallization were required to obtain crystals of suitable quality. Although the initial material was a roughly 1:1 mixture of the ttt and tct isomers, the X-ray structure showed that the crystal contained only the less soluble tct isomer. The ^{1}H NMR spectrum of material from the same recrystallization batch confirmed that only one diastereomer was present. A single peak was observed for each meso proton rather than two as in the original mixture. In addition, the β and CH_2 proton multiplets were less complicated. *ttt*- and *tct*-H_2(OEiBC) have been separated by fractional crystallization[13a] and by chromatography.[17]

Structure Determination of Pd(OEC). A crystal of $C_{36}H_{46}N_4Pd$, Pd(OEC), was cut to size and mounted on a glass fiber. Preliminary Weissenberg photographs exhibited symmetry and systematic absences consistent with the orthorhombic space group *Pnab* (nonstandard setting of *Pbcn*). The crystal was transferred to a Nicolet P3F diffractometer (at Harvard) for data collection. The unit cell was determined by using 23 machine-centered reflections over $20° \le 2\theta \le 33°$. Data were processed with XTAPE of the SHELXTL program package (Nicolet XRD Corp., Madison, WI 53711), and empirical absorption corrections were applied with the program PSICOR. Processed data were transferred to a VAX 8650 computer (Brandeis). All further computational work was carried out using the Enraf-Nonius SDP software package.[18] The analytical scattering factors of Cromer and Waber were employed; real and imaginary components of anomalous scattering were included in the calculations.[19] Other details of the data collection and structure analysis are presented in outline form in Table I. A 2:1 orientational disorder of one of the methyl groups (C12) was treated during the final stages of refinement. The occupancies (0.67 for C12A, 0.33 for C12B) were estimated from a difference Fourier map and held fixed during the refinement. The atom-labeling scheme is shown in the ORTEP diagram (Figure 3). Atomic coordinates for all non-hydrogen atoms appear in Table III. Calculated hydrogen atom positions and thermal parameters are presented in supplementary Table SIII. Anisotropic thermal parameters are given in supplementary Table SIV. Bond lengths and deviations of the non-hydrogen atoms from the Pd–N_4 least-squares plane are summarized in Figure 4. Ranges of bond angles are presented in Table V. Complete bond lengths and angles are given in supplementary Table SV. Least-squares planes and dihedral angles between planes are presented in supplementary Table SVI. Torsion angles are given in supplementary Table SVII.

X-ray Data Collection for Pd(OEP) and Pd(OEiBC). The same general procedures were followed during the collection of the X-ray data for $C_{36}H_{44}N_4Pd$, Pd(OEP), and $C_{36}H_{48}N_4Pd$, Pd(OEiBC). Each crystal was sealed in a glass capillary tube under nitrogen and then optically aligned on a Picker goniostat operated by a Krisel Control diffractometer automation system. A preliminary search of low-angle reflections ($5° \le 2\theta \le 10°$) yielded a sufficient number of reflections in each case to use an autoindexing routine[20] to determine preliminary lattice parameters. From the unrefined orientation matrix, the orientation angles (ω, χ, and 2θ) for 20 higher order reflections were calculated, optimized by the automatic peak-centering algorithm,[21] and least-squares-fit to give the corresponding refined lattice parameters in Table I.

Intensity data were measured with Zr-filtered Mo X-ray radiation ($\lambda(K\alpha_1) = 0.709\,26$ Å, $\lambda(K\alpha_2) = 0.713\,54$ Å) at a takeoff angle of 2°. Each diffraction peak was scanned with a fixed scan rate in the θ–2θ mode with the scan width calculated from the expression $w = A + B \tan \theta$. Background counts were measured at the extremes of each scan with the crystal and detector being stationary. The pulse-height analyzer of the scintillation detector was adjusted to accept 90% of the diffracted peak. During data collection, the intensities of three standard reflections were measured periodically. The integrated intensity, I, and its standard deviation, $\sigma_c(I)$, for each measured peak were calculated from the expressions $I = w(S/t_s - B/t_b)$ and $\sigma_c(I) = w(S/t_s^2 + B/t_b^2)^{1/2}$, where S represents the total scan count measured in time t_s and B is the combined background count in time t_b. The intensity data were corrected for Lorentz–polarization effects, and duplicate reflections were averaged. Further details of the data collection are summarized in Table I.

Structural Analyses of Pd(OEP) and Pd(OEiBC). The positions of the Pd atoms and all of the interior atoms of the octaethylporphyrin ring of Pd(OEP) were interpolated from an E map calculated with MULTAN78[22] on the basis of the phase assignments for the set with the highest figure of merit. Initial coordinates for the Pd atom in Pd(OEiBC) were determined by an analysis of the Harker vectors provided by an unsharpened Patterson map. Approximate coordinates for the remaining non-hydrogen atoms in each compound were obtained from subsequent Fourier summations and were refined with anisotropic thermal parameters. All of the hydrogen atoms were located using difference Fourier calculations which employed only low-angle data with $(\sin\theta)/\lambda < 0.40$ Å^{-1}. Full-matrix least-squares refinement[23-28] (based on F_o^2) of the positional and anisotropic thermal parameters for the 21 independent non-hydrogen atoms and the 22 independent hydrogen atoms of Pd(OEP) led to final discrepancy indices of $R(F_o) = 0.057$, $R(F_o^2) = 0.089$, and

(15) Hoard, J. L. *Ann. N.Y. Acad. Sci.* **1973**, *206*, 18.
(16) Stolzenberg, A. M.; Schussel, L. J. *Inorg. Chem.* **1991**, *30*, 3205.
(17) Sullivan, E. P., Jr.; Grantham, J. D.; Thomas, C. S.; Strauss, S. H. *J. Am. Chem. Soc.* **1991**, *113*, 5264.
(18) Frenz, B. A.; et al. *Program Package SDP*; Enraf-Nonius Corp.: Delft, The Netherlands, and Bohemia, NY, 1986.
(19) Cromer, D. T.; Waber, J. T. *International Tables for X-ray Crystallography*; Kynoch Press: Birmingham, England, 1974; Vol. IV, pp 99–101, 148–150.
(20) The automatic reflection-indexing algorithm is based upon Jacobson's procedure: Jacobson, R. A. *J. Appl. Crystallogr.* **1976**, *9*, 115.
(21) The peak-centering algorithm is similar to that described by Busing: Busing, W. R. In *Crystallographic Computing*; Ahmed, F. R., Ed.; Munksgaard: Copenhagen, 1970; p 319. The ω, χ, and 2θ angles were optimized with respect to the $K\alpha_1$ peak ($\lambda = 0.709\,26$ Å).
(22) Declerq, J. P.; Germain, D.; Main, P.; Woolfson, M. M. *Acta Crystallogr., Sect. A* **1973**, *A29*, 231.
(23) The least-squares refinement[24] of the X-ray diffraction data was based upon the minimization of $\sum w_i|F_o^2 - S^2F_c^2|^2$, where w_i is the individual weighting factor and S is the scale factor. The discrepancy indices and the standard deviation of an observation of unit weight were calculated from the expressions given in the footnotes to Table I.
(24) The scattering factors employed in all of the structure factor calculations were those of Cromer and Mann[25] for the non-hydrogen atoms and those of Stewart et. al.[26] for the hydrogen atoms with corrections included for anomalous dispersion.[27]
(25) Cromer, D. T.; Mann, J. B. *Acta Crystallogr., Sect. A* **1968**, *A24*, 321.
(26) Stewart, R. F.; Davidson, E. R.; Simpson, W. T. *J. Chem. Phys.* **1965**, *42*, 3175.
(27) Cromer, D. T.; Liberman, D. *J. Chem. Phys.* **1970**, *53*, 1891.
(28) The computer programs that were used for the X-ray diffraction data analyses are described in: Nicholson, G. A.; Petersen, J. L.; McCormick, B. J. *Inorg. Chem.* **1980**, *19*, 195.

Table I. Data for X-ray Diffraction Studies of Pd(OEP), *t*-Pd(OEC), and *tct*-Pd(OEiBC)

	Pd(OEP)	*t*-Pd(OEC)	*tct*-Pd(OEiBC)
	Crystal Data at 21 (1) °C		
formula	$C_{36}H_{44}N_4Pd$	$C_{36}H_{46}N_4Pd$	$C_{36}H_{48}N_4Pd$
cryst syst	triclinic	orthorhombic	monoclinic
space group	$P\bar{1}$ (C_i^1; No. 2)	*Pnab* (D_{2h}^{14}; No. 60)[a]	$P2_1/n$ (C_{2h}^5; No. 14)[b]
a, Å	7.809 (5)	8.969 (3)	12.540 (4)
b, Å	9.934 (4)	15.867 (5)	12.745 (3)
c, Å	10.429 (3)	22.117 (7)	20.557 (6)
α, deg	91.05 (2)		
β, deg	98.07 (4)		92.24 (2)
γ, deg	111.05 (4)		
V, Å^3	745.4 (5)	3147.5 (3.0)	3283 (1.5)
Z	1	4	4
fw	639.2	641.2	643.2
ρ_{calc},[c] g/cm^3	1.425	1.353	1.301
cryst size, mm	0.33 × 0.28 × 0.05	0.25 × 0.25 × 0.50	0.33 × 0.25 × 0.35
μ, cm^{-1}	6.47	6.10	5.87
2θ range of centered reflns, deg	30–35	20–33	30–35
	Data Collection and Refinement		
radiation	Zr-filtered Mo Kα	Mo Kα, graphite monochromator	Zr-filtered Mo Kα
scan type	θ–2θ	θ–2θ	θ–2θ
2θ range of measd reflns	5–55	3–50	5–50
reflns measd	$\pm h,\pm k,+l$	$+h,+k,+l$ and $-h,-k,-l$	$\pm h,+k,+l$
scan speed, deg/min	2	vble; 3–30 (t_p/t_b = 1.0)	2.5
scan range, deg	1.1 + 0.9 tan θ	symm; 1.4 + $\Delta(\alpha_2 - \alpha_1)$	1.1 + 0.8 tan θ
no. of reflns measd	3626	5572; 2781 unique	5967
statistical info, R_{av}[d]	0.023	0.031	0.048
std reflns		variations $\leq \pm 3\sigma(I)$ for each of 3 std reflns	
no. of unique data used to refine	3437 [$F_o^2 > 0$]	1671 [$I > 1.96\sigma(I)$]	4005 [$F_o^2 > 3\sigma(F_o^2)$]
transm coeff	0.85–0.97	1.0	1.0
weighting of reflns, p[e]	0.030	0.04	0.025
R[f]	0.057	0.0358[g]	0.056
R_w[f]		0.0430	
$R(F_o^2)$[h]	0.089[i]		0.082
$R_w(F_o^2)$[h]	0.119[i]		0.110
σ_1	2.43[j]	1.21[k]	2.44[j]
no. of variables	407	191	402
data: param ratio	8.44:1	8.75:1	9.96:1

[a] This is a nonstandard setting of space group *Pbcn*; equivalent positions: $\pm(x, y, z)$; $\pm(^1/_2 - x, ^1/_2 + y, ^1/_2 + z)$; $\pm(^1/_2 + x, -y, z)$; $\pm(-x, ^1/_2 - y, ^1/_2 + z)$. [b] This is a nonstandard setting of space group $P2_1/c$; equivalent positions: $\pm(x, y, z)$; $(^1/_2 + x, ^1/_2 - y, ^1/_2 + z)$; $(^1/_2 - x, ^1/_2 + y, ^1/_2 - z)$. [c] ρ_{obs} measured by neutral buoyancy in aqueous CsCl solution agreed within experimental error. [d] For Pd(OEC), $R_{av} = \sum|I - I_{av}|/\sum I$. For others, $R_{av} = \sum|F_o - F_{o,av}|/\sum F_o$. [e] For Pd(OEC), according to: Corfield, P. W. R.; Doedens, R. J.; Ibers, J. A. *Inorg. Chem.* **1967**, *6*, 197. For others, see text. [f] $R = \sum||F_o| - |F_c||/\sum|F_o|$; $R_w = [\sum w(|F_o| - |F_c|)^2/\sum w|F_o|^2]^{1/2}$. [g] $R = 0.074$ for the structure factor calculation with all 2781 reflections. [h] $R(F_o^2) = \sum|F_o^2 - F_c^2|/\sum F_o^2$; $R_w(F_o^2) = [\sum w_i(|F_o^2 - F_c^2|)^2/\sum w_i F_o^4]^{1/2}$. [i] Based on data with $F_o^2 > \sigma(F_o^2)$. [j] $\sigma_1 = [\sum w_i|F_o^2 - F_c^2|/(n - p)]^{1/2}$, where n is the number of observations and p is the number of parameters varied during the last refinement cycle. [k] $\sigma_1 = [\sum w(|F_o| - |F_c|)^2/(m - n)]^{1/2}$, where m (=1671) is the number of observations and n (=191) is the number of parameters.

$R_w(F_o^2) = 0.119$ with $\sigma_1 = 2.43$ for the 3333 reflections with $F_o^2 > \sigma(F_o^2)$. The corresponding anisotropic refinement of the 41 non-hydrogen atoms with varied (H1–H8) or fixed (H9–H48) isotropic temperature factors for the 48 hydrogen atoms of Pd(OEiBC) converged with final discrepancy indices of $R(F_o) = 0.056$, $R(F_o^2) = 0.082$, and $R_w(F_o^2) = 0.110$ with $\sigma_1 = 2.44$ for the 4005 reflections with $F_o^2 > 3\sigma(F_o^2)$. A final difference Fourier summation was calculated in each case and did not reveal any significant regions of residual electron density.

The atom-labeling scheme for Pd(OEP) is shown in the ORTEP diagram (Figure 1). Atomic coordinates for the refined atoms are presented in Table II. Thermal parameters are collected in supplementary Table SI. Bond lengths and deviations of the non-hydrogen atoms from the Pd–N_4 least-squares plane are summarized in Figure 2. Ranges of bond angles are presented in Table V. Complete bond lengths and angles are given in supplementary Table SII.

The atom-labeling scheme for *tct*-Pd(OEiBC) is given in Figure 6. Atomic coordinates for the refined atoms are presented in Table IV. Calculated atomic coordinates for ethyl group hydrogen atoms, H9–H48, are collected in supplementary Table SVIII. Thermal parameters are given in supplementary Table SIX. Bond lengths and deviations of the non-hydrogen atoms from the Pd–N_4 least-squares plane are summarized in Figures 7 and 8, respectively. Ranges of bond angles are presented in Table V. Complete bond lengths and angles are given in supplementary Table SX. Least-squares planes and dihedral angles between planes are presented in supplementary Table SXI.

Results and Discussion

The sites that Pd(OEP), *t*-Pd(OEC), and *tct*-Pd(OEiBC) occupy in their respective lattices have different symmetries. We have adopted an atom-numbering scheme for each molecule that is appropriate to the symmetry imposed by its site. Consequently, each scheme is different.

Structure of Pd(OEP). The palladium atom of Pd(OEP) is located at an inversion center. The structure of the molecule (Figure 1) is entirely typical of porphyrin complexes. The macrocycle bond lengths (Figure 2) and bond angles (Table V) are unremarkable.[29] The Pd–N bond lengths of 2.010 (3) and 2.017 (3) Å are within 3σ of the 2.009 (9) Å Pd–N bond length of Pd(TPP)[30] and are in reasonable agreement with the 2.022 (1) Å Pd–N bond length of [*meso*-tetrakis(3,5-di-*tert*-butyl-4-hydroxyphenyl)porphyrinato]palladium(II).[31] The inversion center imposes strict coplanarity on Pd and the four nitrogen atoms of Pd(OEP). In addition, all macrocycle atoms lie within 0.050 Å of this plane (Figure 2). The CH_2 group carbons of the ethyl substituents are within 0.093 Å of the plane. By way of contrast, Pd(TPP) experiences a large S_4 ruffling distortion which was attributed to interactions with substituents of nearest neighbor molecules.[30]

Two structural features of Pd(OEP) raise the possibility that significant overlap of molecules and π–π interactions can occur

(29) Scheidt, W. R. In *The Porphyrins*; Dolphin, D., Ed.; Academic Press: New York, 1979; Vol. 3, pp 463–511.
(30) Fleischer, E. B.; Miller, C. K.; Webb, L. E. *J. Am. Chem. Soc.* **1964**, *86*, 2342.
(31) Golder, A. J.; Milgrom, L. R.; Nolan, K. B.; Povey, D. C. *J. Chem. Soc., Chem. Commun.* **1987**, 1788.

Table II. Atomic Coordinates for All Atoms of Pd(OEP)[a]

atom	x	y	z
Pd	0.0	0.0	0.0
N1	0.2727 (4)	0.1208 (3)	0.0132 (3)
N2	0.0089 (4)	−0.0995 (3)	−0.1672 (3)
C1	0.3793 (5)	0.2250 (4)	0.1100 (3)
C2	0.5679 (5)	0.2870 (4)	0.0834 (4)
C3	0.5749 (5)	0.2196 (4)	−0.0273 (4)
C4	0.3894 (5)	0.1163 (4)	−0.0723 (3)
C5	0.3349 (5)	0.0256 (4)	−0.1841 (4)
C6	0.1604 (5)	−0.0739 (4)	−0.2294 (3)
C7	0.1103 (5)	−0.1698 (4)	−0.3462 (4)
C8	−0.0718 (6)	−0.2532 (4)	−0.3529 (4)
C9	−0.1346 (5)	−0.2089 (4)	−0.2422 (3)
C10	−0.3133 (5)	−0.2649 (4)	−0.2137 (4)
C11	0.7223 (6)	0.4089 (5)	0.1651 (4)
C12	0.7353 (7)	0.5560 (5)	0.1233 (5)
C13	0.7376 (5)	0.2453 (5)	−0.0975 (5)
C14	0.7446 (7)	0.3457 (6)	−0.2045 (6)
C15	0.2367 (7)	−0.1712 (6)	−0.4409 (5)
C16	0.2327 (15)	−0.0776 (9)	−0.5496 (8)
C17	−0.1908 (7)	−0.3709 (5)	−0.4555 (4)
C18	−0.3203 (9)	−0.3277 (7)	−0.5515 (5)
H1	0.411 (6)	0.028 (5)	−0.228 (4)
H2	−0.371 (7)	−0.324 (5)	−0.256 (5)
H3	0.831 (7)	0.395 (5)	0.161 (5)
H4	0.715 (6)	0.395 (5)	0.244 (5)
H5	0.619 (8)	0.566 (6)	0.127 (5)
H6	0.828 (7)	0.624 (5)	0.167 (5)
H7	0.764 (7)	0.567 (5)	0.035 (6)
H8	0.741 (5)	0.163 (4)	−0.129 (4)
H9	0.837 (7)	0.274 (5)	−0.039 (5)
H10	0.655 (9)	0.329 (6)	−0.260 (6)
H11	0.840 (7)	0.362 (5)	−0.252 (5)
H12	0.756 (7)	0.436 (6)	−0.166 (5)
H13	0.224 (6)	−0.262 (5)	−0.470 (4)
H14	0.343 (8)	−0.142 (5)	−0.405 (5)
H15	0.136 (10)	−0.076 (8)	−0.591 (7)
H16	0.248 (9)	0.009 (7)	−0.527 (6)
H17	0.337 (9)	−0.057 (7)	−0.604 (7)
H18	−0.117 (7)	−0.407 (5)	−0.484 (5)
H19	−0.267 (6)	−0.455 (5)	−0.413 (4)
H20	−0.272 (7)	−0.250 (5)	−0.575 (5)
H21	−0.393 (7)	−0.284 (6)	−0.505 (5)
H22	−0.403 (7)	−0.410 (5)	−0.618 (5)

[a] Numbers in parentheses in this and the following tables are estimated standard deviations in the least significant digit.

Table III. Atomic Coordinates for the Non-Hydrogen Atoms of *t*-Pd(OEC)

atom	x	y	z
Pd	0.250	0.07939 (3)	0.000
N1	0.250	−0.0491 (3)	0.000
N2	0.3745 (4)	0.0804 (2)	−0.0760 (1)
N3	0.250	0.2062 (3)	0.000
C1	0.3202 (6)	−0.1907 (3)	−0.0198 (2)
C2	0.3384 (5)	−0.0993 (3)	−0.0367 (2)
C3	0.4286 (5)	−0.0701 (3)	−0.0816 (2)
C4	0.4407 (5)	0.0128 (3)	−0.1016 (2)
C5	0.5213 (5)	0.0378 (3)	−0.1556 (2)
C6	0.4992 (5)	0.1215 (3)	−0.1621 (2)
C7	0.4089 (5)	0.1487 (3)	−0.1111 (2)
C8	0.3705 (5)	0.2305 (3)	−0.0970 (2)
C9	0.3005 (5)	0.2583 (3)	−0.0456 (2)
C10	0.2832 (5)	0.3445 (3)	−0.0280 (2)
C11	0.3107 (8)	−0.2496 (4)	−0.0770 (3)
C12A	0.299 (1)	−0.3373 (5)	−0.0692 (5)
C12B	0.418 (2)	−0.306 (1)	−0.074 (1)
C13	0.6070 (5)	−0.0208 (3)	−0.1957 (2)
C14	0.5161 (7)	−0.0637 (3)	−0.2437 (2)
C15	0.5508 (6)	0.1778 (3)	−0.2125 (2)
C16	0.4361 (7)	0.1914 (4)	−0.2596 (2)
C17	0.3260 (8)	0.4183 (3)	−0.0674 (3)
C18	0.2120 (9)	0.4394 (4)	−0.1141 (3)

in the lattice. The mean planes of all Pd(OEP) molecules are required to be parallel, owing to the presence of the inversion

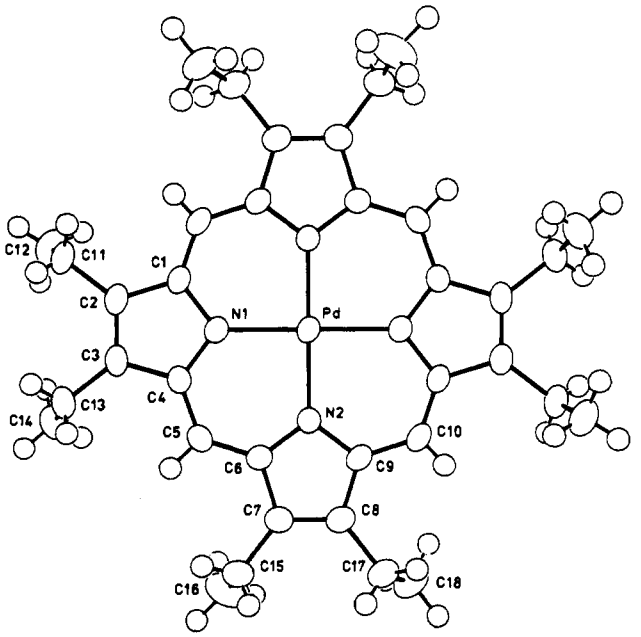

Figure 1. ORTEP diagram of the molecular structure of Pd(OEP), $C_{36}H_{44}N_4Pd$, labeled with the atom-numbering scheme. An inversion center relates the labeled and unlabeled halves of the molecule. Thermal ellipsoids are scaled to enclose 50% probability.

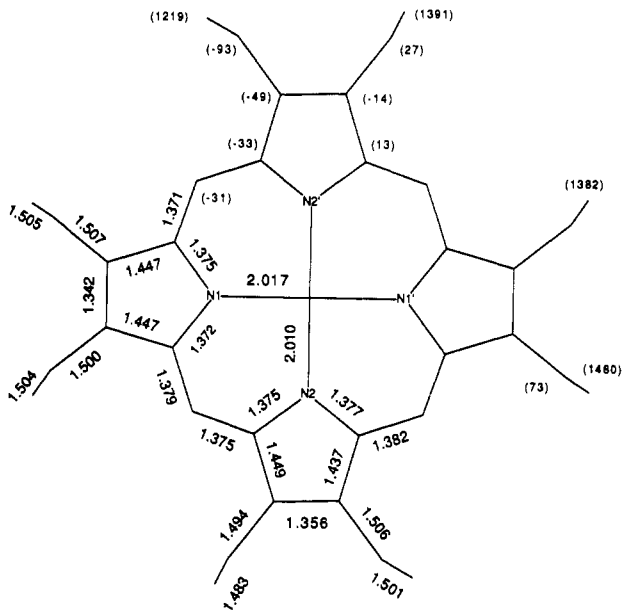

Figure 2. Bond lengths (Å) and deviations (Å × 10^3) from the least-squares plane of Pd and the four nitrogens in Pd(OEP). Typicals esd's in bond lengths and deviations are respectively 0.005 and 0.004 Å for the macrocycle atoms and 0.007 and 0.006 Å for the ethyl group carbons. Deviations smaller than 3σ are not shown.

centers. All four CH_3 groups of the ethyl substituents of the unique half-molecule lie on the same side of the molecule. The symmetry-related half-molecule will have ethyl substituents pointing to the opposite side. Thus, unhindered access to each face of the macrocycle is available around half of the circumference. Packing diagrams (supplementary Figure S1) show that overlap does occur. The region of overlap is roughly a single pyrrole ring. Calculations establish a mean plane separation of 3.47 Å between the pair of closest neighbor molecules, which are related by unit translation along the *a* axis. The closest intermolecular contacts between non-hydrogen atoms of the pair are only slightly longer. The macrocycle carbons C3 and C5 of adjacent molecules are separated by 3.505 Å. Given that the Pd–Pd separation is 7.809 Å, the slip angle and lateral shift of the neighboring molecules are 63.6° and 7.00 Å, respectively. In

Table IV. Atomic Coordinates for All Refined Atoms[a] of *tct*-Pd(OEiBC)

atom	*x*	*y*	*z*
Pd	0.03145 (4)	0.04993 (3)	0.24200 (2)
N1	0.0526 (4)	−0.0471 (4)	0.1662 (2)
N2	0.1454 (4)	0.1466 (4)	0.2088 (2)
N3	0.0118 (3)	0.1466 (4)	0.3192 (2)
N4	−0.0825 (4)	−0.0474 (4)	0.2744 (2)
C1	0.1232 (5)	−0.0371 (5)	0.1182 (3)
C2	0.1992 (6)	0.0432 (6)	0.1170 (3)
C3	0.2097 (5)	0.1272 (5)	0.1567 (3)
C4	0.2965 (6)	0.2090 (5)	0.1543 (4)
C5	0.2550 (6)	0.2968 (6)	0.1945 (4)
C6	0.1724 (5)	0.2411 (5)	0.2337 (3)
C7	0.1304 (6)	0.2852 (6)	0.2885 (3)
C8	0.0592 (5)	0.2402 (5)	0.3286 (3)
C9	0.0205 (6)	0.2967 (6)	0.3876 (3)
C10	−0.0346 (6)	0.2087 (5)	0.4227 (3)
C11	−0.0522 (5)	0.1272 (4)	0.3708 (3)
C12	−0.1208 (5)	0.0451 (6)	0.3748 (3)
C13	−0.1399 (5)	−0.0343 (5)	0.3293 (3)
C14	−0.2171 (5)	−0.1158 (5)	0.3342 (3)
C15	−0.2079 (5)	−0.1778 (5)	0.2813 (3)
C16	−0.1228 (5)	−0.1363 (5)	0.2441 (3)
C17	−0.0876 (6)	−0.1764 (5)	0.1866 (3)
C18	−0.0059 (6)	−0.1375 (5)	0.1505 (3)
C19	0.0316 (6)	−0.1806 (5)	0.0922 (3)
C20	0.1127 (6)	−0.1201 (5)	0.0724 (3)
C21	0.4057 (6)	0.1642 (7)	0.1847 (5)
C22	0.3991 (6)	0.1242 (7)	0.2524 (4)
C23	0.2001 (7)	0.3812 (6)	0.1494 (4)
C24	0.2782 (8)	0.4433 (7)	0.1107 (5)
C25	−0.0614 (7)	0.3850 (6)	0.3669 (4)
C26	−0.0977 (9)	0.4465 (7)	0.4249 (4)
C27	0.0365 (7)	0.1656 (6)	0.4801 (3)
C28	0.0471 (7)	0.2420 (6)	0.5373 (3)
C29	−0.2986 (6)	−0.1236 (5)	0.3853 (3)
C30	−0.3961 (7)	−0.0635 (8)	0.3708 (5)
C31	−0.2659 (5)	−0.2789 (6)	0.2661 (3)
C32	−0.2106 (6)	−0.3742 (5)	0.2926 (4)
C33	−0.0071 (9)	−0.2799 (8)	0.0630 (5)
C34	−0.1080 (15)	−0.2694 (11)	0.0277 (6)
C35	0.1738 (6)	−0.1286 (6)	0.0111 (3)
C36	0.1182 (8)	−0.0801 (8)	−0.0463 (4)
H1	0.243 (5)	0.042 (5)	0.086 (3)
H2	0.293 (6)	0.232 (6)	0.103 (4)
H3	0.318 (5)	0.301 (5)	0.231 (3)
H4	0.166 (5)	0.356 (5)	0.300 (3)
H5	0.086 (5)	0.314 (5)	0.419 (3)
H6	−0.103 (4)	0.228 (4)	0.430 (2)
H7	−0.156 (4)	0.045 (5)	0.404 (3)
H8	−0.127 (4)	−0.237 (5)	0.175 (3)

[a] Atoms H9–H48 of the eight ethyl groups were included as fixed contributions.

Table V. Ranges of Bond Angles (deg)[a]

angle	Pd(OEP)	*t*-Pd(OEC)	*tct*-Pd(OEiBC)
cis N–Pd–N	89.9–90.1 (1)	89.5 (1)	89.6 (2)
cis N–Pd–N_s[b]		90.5 (1)	89.8–90.4 (2)
cis N_s–Pd–N_s			90.2 (2)
trans N–Pd–N	180 (0)[c]	179.1 (1)	
trans N–Pd–N_s		180 (0)[c]	179.1–179.4 (2)
Pd–N–C_a[d]	126.8–127.2 (3)	125.9–127.2 (3)	126.5–127.9 (4)
Pd–N_s–C_{as}		125.0 (2)	125.7–126.2 (4)
C_a–N–C_a	105.7–106.0 (3)	106.4–107.0 (4)	105.1–106.0 (5)
C_{as}–N_s–C_{as}		110.0 (4)	107.9–108.5 (5)
N–C_a–C_b	109.6–110.4 (3)	109.3–110.3 (4)	109.2–111.5 (6)
N_s–C_{as}–C_{bs}		110.2 (4)	110.1–112.7 (6)
N–C_a–C_m	123.8–124.4 (4)	124.1–125.7 (4)	123.1–124.6 (6)
N_s–C_{as}–C_m		124.9 (3)	124.2–125.6 (6)
C_a–C_m–C_a	127.3–127.6 (4)	127.1 (4)	127.7 (6)
C_a–C_m–C_{as}		126.8 (4)	126.9 (6)
C_{as}–C_m–C_{as}			127.7–128.3 (7)
C_m–C_a–C_b	125.4–125.9 (3)	123.9–126.4 (4)	125.4–126.4 (6)
C_m–C_{as}–C_{bs}		124.9 (3)	121.6–125.6 (6)
C_a–C_b–C_b	106.6–107.4 (4)	106.4–107.0 (4)	106.0–108.2 (6)
C_{as}–C_{bs}–C_{bs}		103.3 (4)	101.4–103.4 (6)
C_a–C_b–C_{CH_2}	124.7–125.7 (4)	123.9–125.1 (4)	124.3–125.6 (7)
C_{as}–C_{bs}–C_{CH_2}		112.2 (4)	110.1–110.6 (6)
C_b–C_b–C_{CH_2}	127.7–128.5 (4)	128.2–129.1 (4)	127.3–128.8 (7)
C_{bs}–C_{bs}–C_{CH_2}		114.5 (4)	110.0–111.4 (6)

[a] Numbers in parentheses are the largest observed estimated standard deviation in the least significant digit for the individual angles included in the range. [b] The subscript s designates angles in saturated, pyrroline rings. [c] Imposed by crystallographic symmetry. [d] C_a indicates an α carbon, C_b a β carbon, and C_m a meso carbon.

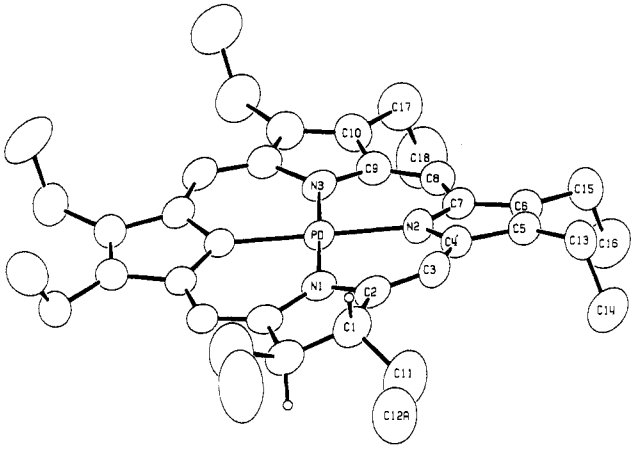

Figure 3. ORTEP diagram of the molecular structure of *t*-Pd(OEC), $C_{36}H_{46}N_4Pd$, labeled with the atom-numbering scheme. A 2-fold axis which passes through N1, Pd1, and N3 relates the labeled and unlabeled halves of the molecule. Thermal ellipsoids are scaled to enclose 50% probability. C12B, the lesser occupied position of the disordered methyl group C12, and hydrogen atoms other than the pyrroline β-H have been omitted for clarity.

the terminology of Scheidt and Lee, these values place Pd(OEP) in group W, the group of tetrapyrrole compounds with weak to nonsignificant π–π interactions in the solid state.[14]

Structure of *t*-Pd(OEC). *t*-Pd(OEC) sits on the crystallographic 2-fold axis ($^1/_4$, *y*, 0) which passes through atoms N1 (pyrroline ring), Pd, and N3 (Figure 3). The orientation of the pyrroline and pyrrole rings is completely ordered with respect to the crystallographic axis. This arrangement is possible because *t*-OEC complexes have intrinsic 2-fold symmetry. However, a 2:1 orientational disorder is observed for the CH_3 group of the pyrroline ring ethyl substituent, C12. In the preferred orientation C12A, shown in Figure 3, the C11–C12 bond is roughly parallel to the crystallographic 2-fold axis. In the minor orientation, the bond is directed outward at an acute angle from the axis.

The bond distances (Figure 4) and bond angles (Table V) are consistent with those observed for other alkyl-substituted hydroporphyrins. The C_a–C_b and C_b–C_b bond lengths in the pyrroline ring are longer than corresponding pyrrole values, which reflects the sp^3 hybridization of the pyrroline C_b carbons. The C_a–N–C_a angle of the pyrroline ring is larger, and the Pd–N–C_a angle is smaller. Pd–N(pyrrole) bonds in Pd(OEC) and Pd(OEP) are of comparable lengths. The Pd–N1(pyrroline) bond length is 2.039 (5) Å, which is ca. 0.025 Å longer than the average length of the Pd–N(pyrrole) bonds.

The 2-fold axis imposes planarity on the palladium and the four nitrogen atoms. The rest of the chlorin macrocycle is significantly S_4 ruffled (Figure 4). The average absolute displacement of the meso carbons from the mean plane of the four nitrogen atoms, d_m, is 0.312 (7) Å. The dihedral angles between the planes of opposite pyrrole rings and the opposite pyrrole and pyrroline ring are 19.3 (4) and 23.1 (4)°, respectively. The pyrroline ring adopts a half-chair configuration with C1 and C1′ 0.100 (5) Å below and above the least-squares plane of the five pyrroline ring atoms. The inclination of the C_b–C_b bond follows that of the S_4 ruffle.

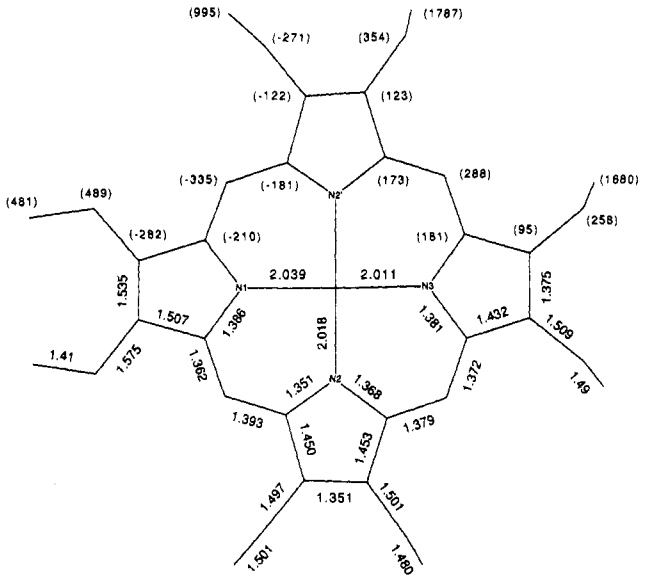

Figure 4. Bond lengths (Å) and deviations (Å × 10^3) from the least-squares plane of Pd and the four nitrogens in *t*-Pd(OEC). Typicals esd's in bond lengths and deviations are 0.006 and 0.005 Å, respectively.

The ethyl substituents are pseudodiequatorial. These conformational features of the pyrroline ring are the same as those preferred in Ni hydroporphyrin complexes, where the S_4 ruffle of the macrocycle is thought to couple to, and control, the conformation of the pyrroline rings.[13] The origin of these features in Pd(OEC), discussed below, appears to be different.

t-Pd(OEC) is nearly isostructural with *t*-Fe(OEC).[11] Both crystallize in the same space group (*Pbcn* for Fe vs the nonstandard setting *Pnab* for Pd), have similar lattice parameters, and have the same orientation of molecules and their substituents with respect to the symmetry elements of the space group. The steepness of the ruffle is somewhat less for Pd(OEC) than for Fe(OEC), which has d_m = 0.40 Å. The S_4 distortion of Fe(OEC) was attributed to the tendency to optimize the M–N distances, which are decreased by this type of distortion.[11] The average Fe–N(pyrrole) distance of 1.976 (6) Å for Fe(OEC) may be less than the corresponding distance of 1.996 (8) Å for Fe(OEP). The Fe–N(pyrroline) distance is only 0.01 Å longer than the average Fe–N(pyrrole) bond distance in Fe(OEP) and lies between the two individual values. The S_4 distortion of Pd(OEC) cannot be rationalized on the basis of reducing the M–N distances. The Pd–N distances are some 0.1–0.3 Å longer than the Fe–N distances in the corresponding complexes. Furthermore, Pd–N distances in Pd(OEC) are all greater than or equal to the Pd–N distances in Pd(OEP).

The reason for the S_4 distortion of Pd(OEC) is suggested by an examination of its packing (Figure 5). The molecule centered at ($^1/_4$, 0.079, 0) overlaps over half its diameter with a second molecule centered at ($^3/_4$, −0.079, 0). There is an equivalent interaction with a third molecule centered at ($^{-1}/_4$, −0.079, 0), which is related to the second molecule by a unit translation along the *a* axis. These interactions generate an infinite stack of overlapping molecules. The stack propagates along the *a* axis with mean planes inclined 146.4° to the axis. The other molecules in the unit cell are in similar stacks. Those on the ($\pm^1/_4$, *y*, $^1/_2$) 2-fold axes have mean planes inclined 33.6° to the *a* axis. The stacks are arranged in a herringbone pattern when viewed down the *b* axis (supplementary Figure S2). The mean plane separation between molecules in these stacks is 3.735 Å, but the closest intermolecular contacts between non-hydrogen atoms are substantially shorter. The distance from Pd to meso carbon C3 in the adjacent molecule is 3.405 Å, which is only 0.005 Å greater than the distance of C3 from the mean plane of the first molecule. Thus, C3 in the adjacent molecule is almost directly above Pd in the first molecule and is only about 0.01 Å further from it than the meso carbons in the first molecule. Other close contacts between macrocycle atoms in neighboring molecules include N2–C2, 3.597 Å, and N1–C4, 3.617 Å. Several contacts less than 3.7 Å are observed for ethyl group carbons, particularly for C12B, the minor orientation of the disordered pyrroline ring ethyl group. Interestingly, meso carbons C3 and C8 are the macrocycle carbons which experience the largest deviation from the mean plane as a result of the S_4 ruffle. The S_4 ruffle of Pd(OEC) results in significantly shorter contacts between C3 and a neighboring Pd atom than would have occurred if the molecules were planar or ruffled in the enantiomerically related sense. The S_4 ruffle and associated half-chair conformation of the pyrroline ring also result in decreased steric interactions between adjacent molecules and the pyrroline ring ethyl substituents, which lie inside the region of overlap. The inclination of the pyrroline C_b–C_b bond and its resulting pseudodiequatorial conformation direct the ethyl groups along the 2-fold axis away from adjacent molecules. The ethyl groups would be pseudeodiaxial and directed toward adjacent molecules if Pd(OEC) were planar or if the inclination of the pyrroline C_b–C_b bond relative to the ruffle were reversed. Thus, optimization of intermolecular interactions in the solid state appears to be responsible to a large degree for the S_4 ruffle and overall conformation of Pd(OEC).

Steric interactions between peripheral substituents and the half-chair conformation of the pyrroline ring are other potential

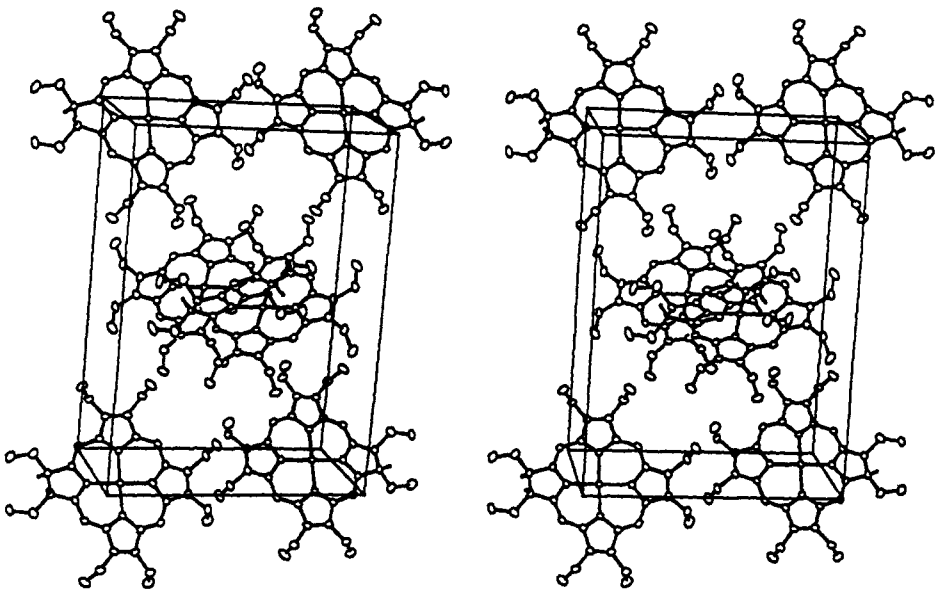

Figure 5. Stereoview of packing in the unit cell of Pd(OEC). The *b* axis is horizontal, and the *c* axis is vertical.

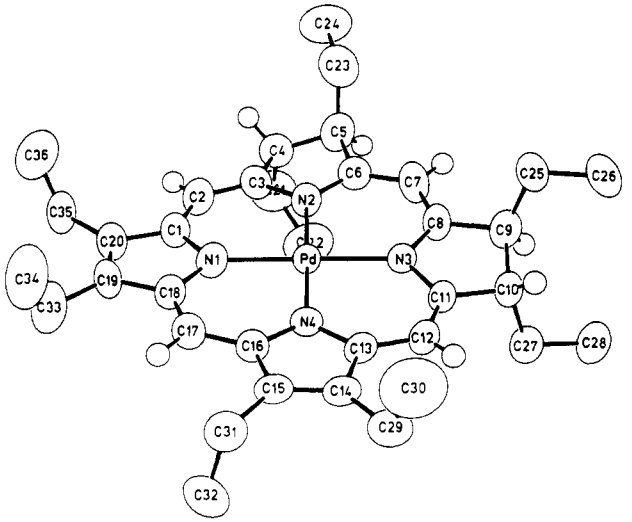

Figure 6. ORTEP diagram of the molecular structure of *tct*-Pd(OEiBC), $C_{36}H_{48}N_4Pd$, labeled with the atom-numbering scheme. C21 and C22 are obscured in this view. Thermal ellipsoids are scaled to enclose 50% probability. The hydrogen atoms on the ethyl groups have been omitted for clarity.

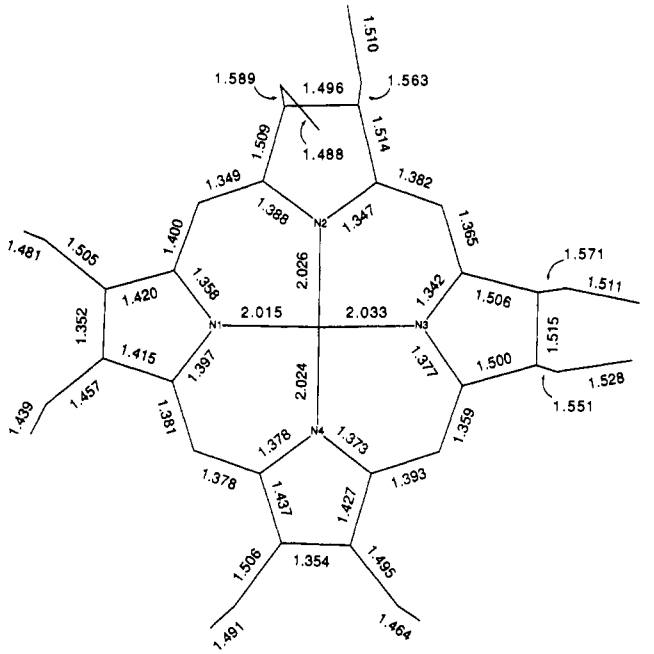

Figure 7. Bond lengths (Å) for *tct*-Pd(OEiBC). Typicals esd's are 0.005 Å for Pd–N bonds, 0.009 Å for bonds between macrocycle atoms, and 0.012 Å for bonds between ethyl group carbons.

factors that could contribute to the observed ruffled conformation, even in the absence of intermolecular interactions. The significance of these factors cannot be evaluated by comparisons of the structures of *t*-Pd(OEC) and free-base *t*-H_2(OEC) because the X-ray structure of the latter has not been reported. However, structures of the free bases *tct*- and *ttt*-H_2(OEiBC) are available.[13a] The tct isomer, in which the 3- and 7-ethyl substituents are on the same side of the macrocycle and are potentially in contact, is ruffled in both the free-base and Pd structures, discussed below. In contrast, the free-base ttt isomer, which has the 3- and 7-ethyl substituents on opposite sides of the macrocycle, is planar. It would appear, then, steric interactions between peripheral substituents and the half-chair conformation of the pyrroline ring can cause ruffling in some cases but do not require ruffling in all cases. We do not believe that these factors play the dominant role in determining the conformation of Pd(OEC). Consistent with this conclusion, Pd(OEC) is not ruffled in solution on the NMR time scale. Its ^1H and ^{13}C NMR spectra[16] do not exhibit the distinctive features which confirmed the ruffled conformation of Ni(OEC) in solution.[32]

The Pd–Pd separation in the Pd(OEC) stacks is 5.144 Å. Calculations establish that the lateral shift is 3.537 Å and the slip angle is 43.4°. Not surprisingly, these parameters place Pd(OEC) in group I, the group of tetrapyrrole compounds with intermediate-strength π–π interactions in the solid state.[14] The mean plane separation and lateral shift of Pd(OEC) are somewhat larger than those of Fe(OEC),[14] which probably reflects the larger radius of palladium compared to iron. In light of the above discussion, the similarity of the parameters suggest that intermolecular interactions in the solid state could also contribute to the S_4 ruffle of Fe(OEC).

Structure of *tct*-Pd(OEiBC). *tct*-Pd(OEiBC) (Figure 6) occupies a general lattice position. The molecule can have as high as mirror point symmetry. Although the lattice does not impose any symmetry on the molecule, the bond lengths (Figure 7) and angles show approximate mirror symmetry about a plane passing through meso carbons C17 and C7. Chemically equivalent macrocycle bonds differ in length by less than 0.02 Å. Bond lengths and angles (Table V) are typical of hydroporphyrin compounds.

An alternation of long and short bonds around the entire conjugation pathway of Pd(OEiBC) is clearly evident in Figure 7. A similar pattern has been observed in the structures of the isobacteriochlorins H_2(OMiBC)[12,33] Ni(TMiBC)[10c] and to a lesser extent in the chlorin Ni(TMC).[10b] It is absent in Pd(OEC). The alternation was taken as an indication of diminished π-delocalization in these compounds.[10] Others[12] suggest that the alternation and the approximate mirror symmetry reflect a hybrid of the two resonance[34] forms:

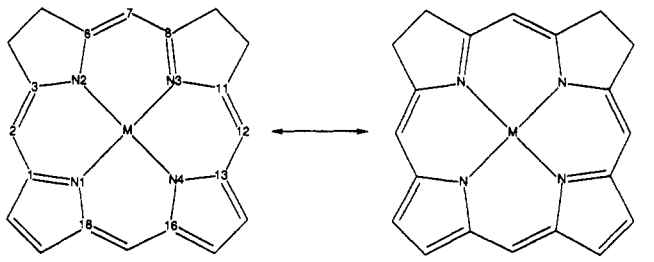

The C3–N2 and C11–N3 bonds are formally single in both resonance forms, while the bonds C6–N2 and C6–C7 and their respective mirror equivalents C8–N3 and C7–C8 are alternately single and double and thus shortened in the hybrid structure. Similarly, bonds C1–C2, C18–N1, and their equivalents are also formally single in both resonance forms, while bond C2–C3 and its equivalent are double bonds in both.

The symmetry of the lattice site does not impose coplanarity on palladium and the four nitrogen atoms of Pd(OEiBC). Nonetheless, the atoms are close to coplanar. N1 and N3 are barely 3σ below the least-squares plane defined by the five atoms (Figure 8). The molecule as a whole is S_4 ruffled, but the distortion is not pronounced. The d_m value is only 0.153 Å, less than half that in Pd(OEC). The average dihedral angle between the planes of the opposite pyrrole and pyrroline rings is 12.0°. The deviations from planarity are substantially larger in the pyrroline rings than in the pyrrole rings. The pyrroline rings adopt half-chair conformations with C_b's roughly 0.125 Å below and

(32) Stolzenberg, A. M.; Stershic, M. T. *Inorg. Chem.* **1987**, *26*, 1970.

(33) Abbreviations: C_a, α carbon; C_b, β carbon; C_m, meso carbon; Ct, center or equivalently the average of the four N donor atoms' coordinates; OMiBC, 2,2,8,8,12,13,17,18-octamethylisobacteriochlorin dianion; OEPC, 2,3,7,8,12,13-hexahydro-2,3,7,8,12,13,17,18-octaethylporphyrin dianion; TMP, 5,10,15,20-tetramethylporphyrin dianion; TMC, 2,3-dihydro-5,10,15,20-tetramethylporphyrin dianion; TMiBC, 2,3,7,8-tetrahydro-5,10,15,20-tetramethylporphyrin dianion; TPyP, 5,10,15,20-tetra-4-pyridylporphyrin dianion; TPC, 2,3-dihydro-5,10,15,20-tetraphenylporphyrin dianion; TPiBC, 2,3,7,8-tetrahydro-5,10,15,20-tetraphenylporphyrin dianion; TPBC, 2,3,12,13-tetrahydro-5,10,15,20-tetraphenylporphyrin dianion.

(34) For the free base H_2(OMiBC),[12] the two forms are tautomers.

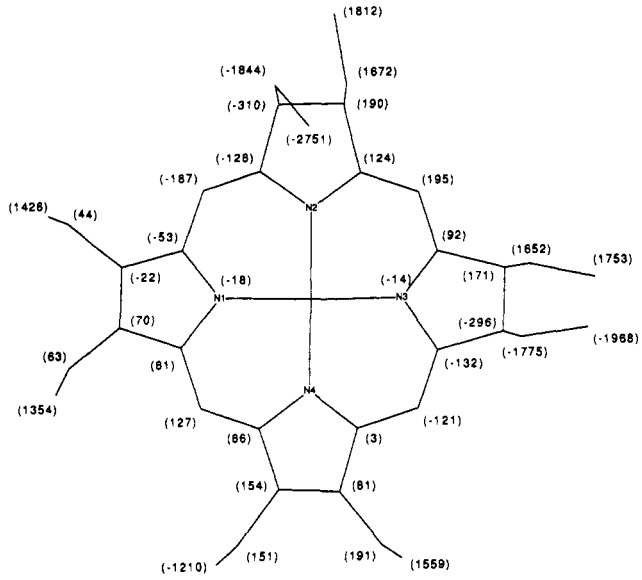

Figure 8. Deviations (Å × 10^3) from the least-squares plane of Pd and the four nitrogens in *tct*-Pd(OEiBC). Typicals esd's are 0.005 Å for N atoms, 0.007 Å for macrocycle carbons, and 0.010 Å for ethyl group carbons. Deviations smaller than 3σ are not shown.

above the least-squares plane of the five atoms of the pyrroline ring. Adjacent meso carbons are displaced from this plane by ±0.16–0.26 Å, which suggests that the pyrroline C_a carbons are pyramidalized to some extent. The inclinations of the C_b–C_b bonds follow that of the S_4 ruffle. Pyrroline ethyl substituents are pseudodiaxial. In general, the conformation of *tct*-Pd(OEiBC) resembles that of the free base *tct*-H_2(OEiBC)[13a] but the Pd complex is more nearly planar.

Interactions between neighboring molecules of Pd(OEiBC) are generally unremarkable (supplementary Figure S3). The shortest non-hydrogen atom intermolecular contacts involving the 25 macrocycle atoms are with ethyl group carbons, and are all longer than 3.61 Å. The mean plane separation between the closest near parallel neighbors is in excess of 4.90 Å. Packing interactions explain one apparently unusual feature, though. Methyl carbon C22 tucks in under the macrocycle to avoid contact with ethyl group C25–C26 on an adjacent molecule.

Core Size Trends. The coordination geometry and macrocycle conformation of the palladium complexes described in this paper differ from those of structurally characterized hydroporphyrin complexes of other metals. The palladium complexes represent a class of square-planar metalloporphyrin and -hydroporphyrin complexes that has M–N distances close to the 2.010 Å value of the idealized reference porphyrin of least strain.[35] The conformations of the macrocycles are planar or slightly ruffled. When observed, ruffled conformations appear to result from packing or an intrinsic ligand conformation that is a consequence of steric interactions between peripheral substituents. *meso*-Tetramethyl-[11] and octaethyl-substituted[13,36] nickel complexes are square planar but, owing to the small radius of Ni(II), have extensively S_4-ruffled macrocycles and short M–N distances. Tetraphenyl-substituted Zn(hydroporphyrinate)(pyridine) complexes are five-coordinate. Because of its coordination number and relatively large radius, Zn is displaced 0.3–0.4 Å above the macrocycle, which is slightly saddle-shaped. In each of the three classes, structural data currently exist for series of identically substituted complexes at three or more levels of macrocycle saturation.

Trends relating to the macrocycle core size were not clearly defined in previous work. Elongation of the pyrroline M–N or Ct–N distances compared to the corresponding pyrrole distances in the same compound is typical of hydroporphyrin compounds. In Ni and Fe hydroporphyrin complexes, the pyrroline M–N distance of one compound is similar to the pyrrole M–N distance in the next most unsaturated compound in the series. The S_4-ruffling distortion complicates comparison between compounds because it results in a reduction in the length of *all* M–N bond distances. Hoard has given a quantitative treatment of the effects of ruffling.[35] On the basis of this model, others have argued that if the ruffled compounds were planar, the pyrroline M–N distances would actually be longer than the pyrrole M–N distances in more unsaturated compounds.[10,11,14] By extension, it was concluded that hydroporphyrins have intrinsically larger core sizes than porphyrins.[10,11] Scheidt observed that the differences in pyrrole M–N and pyrroline M–N distances within a compound become less pronounced as the number of reduced rings increases.[14] The generality of this observation is uncertain, because the examples on which it was based are mostly nickel complexes. Ruffling, which becomes more pronounced in the Ni series as the number of reduced rings increases, is expected to minimize the differences between M–N bond lengths.

The Pd–N distances in Pd(OEC) and Pd(OEiBC) conform to previous observations about M–N distances in hydroporphyrin complexes. The pyrroline Pd–N distance is significantly longer than the pyrrole Pd–N distances in Pd(OEC). The precision of the Pd(OEiBC) structure is too low for the difference between the average pyrroline and pyrrole Pd–N distances (given below) to be significant (>3σ). The Pd–N distances appear to support the arguments for an increase in pyrroline M–N bond distances and core size in nonruffled complexes, even though the Pd hydroporphyrin complexes are slightly ruffled. Average pyrrole Pd–N distances in Pd(OEP), Pd(OEC), and Pd(OEiBC) are 2.014 (4), 2.016 (4), and 2.020 (6) Å, respectively. The pyrroline Pd–N distances are 2.039 (4) and 2.030 (5) Å (average), in the last two complexes, respectively. The pyrroline Pd–N distances of both hydroporphyrins are longer than the pyrrole Pd–N distance of Pd(OEP). Similar trends are observed for the Zn tetraphenyl series of complexes. Except for one short 2.087 (3) Å pyrroline Zn–N distance in TPiBC, which might be underestimated due to disorder,[14] all pyrroline Zn–N distances are longer than 2.115 Å, the average value when the short distance is included.[9] (The average increases to 2.123 (8) Å if this short distance is excluded.) Pyrrole Zn–N distances range from 2.036 (4) to 2.079 (3) Å and average 2.060 (14) Å in the hydroporphyrins, which is not significantly different from the average of 2.073 (8) Å in Zn(TpyP)py.[37] These observations might not provide compelling evidence for core expansion because the displacement of Zn from the macrocycle plane affords other degrees of freedom that can affect the Zn–N distances.

The differences in pyrrole M–N and pyrroline M–N distances within a compound become less pronounced in the palladium series as the number of reduced rings increases. The fundamental correlation of the observed trend may not be with the number of reduced rings, though. It may instead reflect the varying ease with which different hydroporphyrins can distribute the structural perturbation that results from increasing the pyrroline M–N distances over the entire macrocycle. Interestingly, the recently reported structure of Zn(TPBC)(py) violates the generalization.[9c] The pyrroline and pyrrole Zn–N distances in this compound are 2.122 (4) and 2.043 (4) Å, respectively. The difference is greater than in any other hydroporphyrin compound.

The nonbonded distances Ct–C_a and Ct–C_m are two other potential measures of the core size. A purely mechanical model of the porphyrin skeleton predicts that these distances are sensitive to the M–N or Ct–N distance.[37] The average values of the Ct–C_a and Ct–C_m parameters do not change with saturation level in the Pd octaethyl and Zn tetraphenyl series of complexes, both of which have relatively long Ct–N distances. In ruffled complexes, the average Ct–C_a distance appears to decrease with increasing saturation of the macrocycle, but the differences are too small to be significant.

(35) Hoard, J. L. *Ann. N.Y. Acad. Sci.* **1973**, *206*, 18.
(36) (a) Cullen, D. L.; Meyer, E. F., Jr. *J. Am. Chem. Soc.* **1974**, *96*, 2095. (b) Brennan, T. D.; Scheidt, W. R.; Shelnutt, J. A. *J. Am. Chem. Soc.* **1988**, *110*, 3919.
(37) Collins, D. M.; Hoard, J. L. *J. Am. Chem. Soc.* **1970**, *92*, 3761.
(38) Lauher, J. W.; Ibers, J. A. *J. Am. Chem. Soc.* **1973**, *95*, 5148.

Table VI. Comparisons of Molecular Volumes and Crystal Densities

compd	T, K	vol, Å³/ molecule	% change	density, g/cm³	ref
Pd(OEP)	294	745.5		1.425	this work
t-Pd(OEC)	294	786.9	5.6	1.353	this work
tct-(OEiBC)	294	820.7	10.1	1.301	this work
Zn(TPC)py·C_6H_6	nr[a]	1066.5		1.3[b,c]	9a
Zn(TPBC)py·py	298	1065.5		1.31	9c
Zn(TPiBC)py·C_6H_6	nr	1064.3		1.31[b,c]	9b
Ni(OEP), triclinic[d]	293	743.0		1.32	36a
Ni(OEP), tetragonal[e]	293	771.3	3.8	1.27	36a
Ni(OEP), triclinic 2[e]	294	779.8	4.9	1.26	36b
ttt-Ni(OEiBC)	nr	790.6	6.4	1.26	13a
tct-Ni(OEiBC)	nr	791.0	6.5	1.26	13a
ccccc-Ni(OEPC)	113	804.8	8.3	1.23[b]	13d
tctcc-Ni(OEPC)	nr	805.1	8.4	1.23	13b
Ni(TMP)	140	439.4		1.6	10b
Ni(TMC)	123	453.8	3.3	1.56	10b
Ni(TMiBC)[f]	204	475.0	8.1	1.486	10c
Fe(OEP)	293	781.1		1.255	11b
Fe(OEC)	123	739.1	−5.4	1.33	11b
H_2(OEP)	nr	745.2		1.191	38
ttt-H_2(OEiBC)	nr	819.5	10.0	1.1	13a
tct-H_2(OEiBC)	nr	845.9	13.5	1.06	13a
ccctc-H_2(OEPC)	103	787.0	5.6	1.146	13

[a] Temperature of data collection not reported. [b] Recalculated from unit cell parameters. [c] Reported density is 1.25. [d] Planar. [e] S_4 ruffled. [f] Average for the two independent molecules per unit cell.

Trends in Densities. A notable feature of the palladium structures is the steady decrease in density of the crystal with increasing saturation of the macrocycle. Equivalently, the volume occupied per molecule increases with increasing saturation. Because bulk densities are affected by packing defects and the measurement temperature, among other factors, they are not necessarily direct measures of molecular properties. A search of the literature reveals that, despite these uncontrolled factors, the above trend is reasonably general. Table VI compares the molecular volume and crystal densities of several series of porphyrin and hydroporphyrin compounds which crystallize in lattices that have either no solvation or similar solvation. Two exceptions to the trend are the complexes in the Zn tetraphenyl series, which have constant molecular volume and density, and Fe(OEP), which is somewhat less dense than Fe(OEC). (The volume per molecule of Fe(OEP) is 5% larger than that of either Pd(OEP), triclinic Ni(OEP), or H_2(OEP), which all have comparable volumes.) The ruffled and planar phases of Ni(OEP) are included for purposes of comparison.

What could cause the increase in volume occupied per molecule? Kitaigorodskii has shown that organic molecules tend to pack in crystals as closely as their geometry allows.[39] In general, molecules with less regular shapes fill space less efficiently. Hydrogenation of a β-substituted porphyrin lifts the substituents out of the molecular plane and creates a chiral center. The increased conformational freedom of these substituents and of the pyrroline ring results in structures that are less regular than a planar porphyrin. Consequently, the volume occupied per molecule increases by more than just the volume of the additional hydrogen atoms. Ruffling would appear to have a similar effect. The volumes of ruffled tetragonal Ni(OEP) and triclinic-2 Ni(OEP) are 4–5% greater than the planar triclinic Ni(OEP) phase. In contrast, addition of a second hydrogen to a β carbon of TPP would not be expected to have much of an effect on the orientation of the adjacent meso phenyl substituent or the overall shape of the molecule.

The increase in the volume occupied per molecule with saturation could be chemically significant. Hydroporphyrin compounds should have less negative lattice energies and, as a consequence, increased solubility. This is consistent with our experience. Furthermore, to the extent that interactions with neighboring molecules in a lattice model interactions with the surface of a protein binding pocket, the energetics and dynamics of the interactions between a hydroporphyrin prosthetic group and its protein environment could be altered relative to a porphyrin prosthetic group.

Acknowledgment. We thank Professor Richard H. Holm for graciously providing access to his group's diffractometer at Harvard and to Drs. Michel Carrie, Stefano Ciurli, and Hans Kruger for assistance in collecting the Pd(OEC) data set. We thank the National Institutes of Health (Grant GM 33882) for support of this research.

Supplementary Material Available: Figures S1–3, showing stereoviews of packing in the unit cells of Pd(OEP), Pd(OEC), and Pd(OEiBC), and Tables SI–SXI, giving thermal parameters for Pd(OEP), bond lengths and angles for Pd(OEP), atomic coordinates for the hydrogen atoms of Pd(OEC), anisotropic thermal parameters for Pd(OEC), bond lengths and angles for Pd(OEC), least-squares best planes for Pd(OEC), torsion angles for Pd(OEC), atomic coordinates for atoms H9–H48 of Pd(OEiBC), thermal parameters for Pd(OEiBC), bond lengths and angles for Pd(OEiBC), and least-squares best planes for Pd(OEiBC) (32 pages); listings of observed and calculated structure factors for Pd(OEP), Pd(OEC), and Pd(OEiBC) (36 pages). Ordering information is given on any current masthead page.

(39) Kitaigorodskii, A. I. *Organic Chemical Crystallography*; Consultant Bureau: New York, 1955.